A TWO-LAYER PRIMITIVE EQUATION OCEAN CURRENT MODEL AND ITS SIMULATION①

Yang Bo (杨 波) and Qian Yongfu (钱永甫)

Department of Atmospheric Sciences, Nanjing University, Nanjing, 210008

Received 3 July 1995, accepted 6 March 1996

ABSTRACT

A two-layer primitive equation model is developed in this paper. The capabilities of this model are tested by the use of multiyearly averaged January and July sea surface level pressure fields and wind fields which can be diagnosed from the pressure fields. The results show that the ocean surface currents and undercurrents in the second layer driven by the sea surface wind and the sea surface pressure are close to the observation. The results are also compared with that of the IAP OGCM and the OSU OGCM.

Key words: ocean circulation model, numerical simulations

I. INTRODUCTION

The world ocean is one of the important components of the climate system. It has two significant features: wide time scale and grand thermal and dynamic inertia. In order to predict climate over more than several decades, the entire ocean, including the deep sea, should be considered. However, as to short-term climate variation, we can divide the whole process into two parts: the dynamic process and thermal process, the former is an active process while the latter is a passive one.

In this paper, we developed a two-layer primitive equation model based on earlier work (Qian and Wang, 1994). At first, multiyearly averaged January and July sea surface level pressure fields and wind fields which can be diagnosed from the pressure fields are used to set up this model to simulate the main features of currents in winter and summer. If the result is good, we can use this model to do some research work on short term climate variation.

From the view point of dynamics, most of the widely used general circulation models are based on simplified primitive equations in which the surface gravitational wave has been filtered through rigid-lid simplification. Such oceanic models are very similar to the integral nondivergent atmosphere model used in the early stage of numerical weather prediction. Meteorologists have pointed out using theoretical analysis and experiments that this hypothesis can cause too much backward extra-long waves.

Because of the small scale of Rossby radius of deformation in ocean and the grand meridionality of the movement of the ocean water, most of the maelstroms and longer waves in the ocean belong to ultra-long waves. So governing equation using nondivergent simplification may distort the structure and propagation properties of these waves. Zeng (1983) also pointed out that governing equations including integral nondivergent simpli-

① This paper was jointly supported by the National Key Project of Fundamental Research, Climate Dynamics and Theoretical Study on Climate Predictability and the National Natural Science Foundation of China.

fication eliminated "available potential energy" and the lack of mechanism of transformation between available potential energy and dynamic energy distorted the real picture of energy transformation and energy circulation (Zeng, Yuan and Zhao et al., 1992).

Based on the analysis given above, Zeng (1983) eliminated the unreasonable rigid-lid simplification and introduced free sea height as a predictand. In this paper we also consider sea surface height variations. Sea surface is a free surface and its height can be predicted with the equation of continuity. From the view point of dynamics, sea surface height variation plays an important role in the gradient field. We can calculate the main features of water movements based on it in the upper layer and the second layer. Thus it has important applications on ocean dynamics and large scale air-sea interaction.

II. COMPUTATIONAL DESIGN OF THE MODEL

The model ocean is divided into two unequivalent parts at vertical axis. $H_1 = 50\text{m}$, $H_2 = 200\text{ m}$, $H_1 + H_2 = 250\text{ m}$. Let the vertical velocity between two layers be W_b. The upward direction is defined as positive direction. We can describe the movement of water in the upper layer using the following equations:

$$\frac{\partial \eta}{\partial t} + \nabla \cdot (H_1 + \eta)\vec{V}_1 = W_b \tag{1}$$

$$\frac{\partial u_1}{\partial t} + \vec{V}_1 \cdot \nabla u_1 = -\frac{1}{\rho_0}\frac{\partial p_s}{\partial x} - g\frac{\partial \eta}{\partial x} + fv_1 + A_m \Delta u_1 + (\tau_{ax} - \tau_{bx})/\rho_0(H_1 + \eta) \tag{2}$$

$$\frac{\partial v_1}{\partial t} + \vec{V}_1 \cdot \nabla v_1 = -\frac{1}{\rho_0}\frac{\partial p_s}{\partial y} - g\frac{\partial \eta}{\partial y} - fu_1 + A_m \Delta v_1 + (\tau_{ay} - \tau_{by})/\rho_0(H_1 + \eta). \tag{3}$$

η is the free sea surface height. P_s is the sea level pressure. u_1 and v_1 are the horizontal sectors of the velocities of ocean surface currents. f is the Coriolis parameter. A_m is the momentum diffusion coefficient. τ_a and τ_b are the frictional stress between air and sea and between two layers respectively.

The form of shearing stress is given as follows:

$$\vec{\tau}_a = \rho_a C_D |\vec{V}_a| (\vec{V}_a - \vec{V}_1) \tag{4}$$

$$\vec{\tau}_b = \rho_0 e |\vec{V}_1| (\vec{V}_1 - \vec{V}_2). \tag{5}$$

Let the subscript "a" represent the values in atmosphere near the surface of water.

As to the movement of water in the second layer, when we suppose that the vertical velocity at the bottom of this layer is equal to zero, we have the following equations:

$$\nabla \cdot H_2 \vec{V}_2 + W_b = 0 \tag{6}$$

$$\frac{\partial u_2}{\partial t} + \vec{V}_2 \cdot \nabla u_2 = -\frac{1}{\rho_0}\frac{\partial p_s}{\partial x} - g\frac{\partial \eta}{\partial x} + fv_2 + A_m \Delta u_2 + (\tau_{bx} - \tau_{dx})/\rho_0 H_2 \tag{7}$$

$$\frac{\partial v_2}{\partial t} + \vec{V}_2 \cdot \nabla v_2 = -\frac{1}{\rho_0}\frac{\partial p_s}{\partial y} - g\frac{\partial \eta}{\partial y} - fu_2 + A_m \Delta v_2 + (\tau_{by} - \tau_{dy})/\rho_0 H_2. \tag{8}$$

Let the bottom friction have the following form:

$$\vec{\tau}_d = \rho_0 e |\vec{V}_2| \vec{V}_2. \tag{9}$$

The Coriolis force term and stress term are treated with implicit scheme. Other terms are treated with explicit scheme. Let Δt be the time step. Then we have difference equations as follows:

$$\hat{\beta}_1 u_1^{(t+1)} - \hat{f}_1 v_1^{(t+1)} = A_1 \tag{10}$$

$$\hat{f}_1 u_1^{(t+1)} + \hat{\beta}_1 v_1^{(t+1)} = A_2 \tag{11}$$

$$A_1 = -\frac{1}{\rho_0}\frac{\partial p_s}{\partial x}\cdot dmt - g\frac{\partial \eta^{(t)}}{\partial x}\cdot dmt - \vec{V}_1\cdot\nabla u_1^{(t)}\cdot dmt + A_m\Delta u_1^{(t)}\cdot dmt$$
$$+\frac{\rho_a}{\rho_0}C_D\frac{|\vec{V}_a|}{H_1+\eta^{(t)}}u_a\cdot dmt + \frac{\varepsilon}{H_1+\eta^{(t)}}|\vec{V}_1|u_2^{(t)}\cdot dmt + u_1^{(t)} \tag{12}$$

$$A_2 = -\frac{1}{\rho_0}\frac{\partial p_s}{\partial y}\cdot dmt - g\frac{\partial \eta^{(t)}}{\partial y}\cdot dmt - \vec{V}_1\cdot\nabla v_1^{(t)}\cdot dmt + A_m\Delta v_1^{(t)}\cdot dmt$$
$$+\frac{\rho_a}{\rho_0}C_D\frac{|\vec{V}_a|}{H_1+\eta^{(t)}}v_a\cdot dmt + \frac{\varepsilon}{H_1+\eta^{(t)}}|\vec{V}_1|v_2^{(t)}\cdot dmt + v_1^{(t)} \tag{13}$$

$$\hat{\beta}_1 = 1 + \left(\frac{\rho_a}{\rho_0}C_D\frac{|V_a|}{H_1+\eta^{(t)}} + \frac{\varepsilon}{H_1+\eta^{(t)}}|\vec{V}_1|\right)\cdot dmt \tag{14}$$

$$\hat{f}_1 = f\cdot dmt. \tag{15}$$

The same operation is done to the equations for the second layer, and we get

$$\hat{\beta}_2 u_2^{(t+1)} - \hat{f}_2 v_2^{(t+1)} = B_1 \tag{16}$$

$$\hat{f}_2 u_2^{(t+1)} + \hat{\beta}_2 v_2^{(t+1)} = B_2 \tag{17}$$

$$B_1 = -\frac{1}{\rho_0}\frac{\partial p_s}{\partial x}\cdot dmt - g\frac{\partial \eta^{(t)}}{\partial x}\cdot dmt - \vec{V}_2\cdot\nabla u_2^{(t)}\cdot dmt + A_m\Delta u_2^{(t)}\cdot dmt$$
$$+\frac{\varepsilon}{H_2}|\vec{V}_1|u_1^{(t+1)}\cdot dmt + u_2^{(t)} \tag{18}$$

$$B_2 = -\frac{1}{\rho_0}\frac{\partial p_s}{\partial y}\cdot dmt - g\frac{\partial \eta^{(t)}}{\partial y}\cdot dmt - \vec{V}_2\cdot\nabla v_2^{(t)}\cdot dmt + A_m\Delta v_2^{(t)}\cdot dmt$$
$$+\frac{\varepsilon}{H_2}|\vec{V}_1|v_1^{(t+1)}\cdot dmt + v_2^{(t)} \tag{19}$$

$$\hat{\beta}_2 = 1 + \left(\frac{\varepsilon}{H_2}|\vec{V}_1| + \frac{\varepsilon}{H_2}|\vec{V}_2|\right)\cdot dmt \tag{20}$$

$$\hat{f}_2 = f\cdot dmt. \tag{21}$$

As to Eq. (1), do the following transformation, then we get

$$\frac{\partial \eta}{\partial t} + (H_1+\eta)\nabla\cdot\vec{V}_1 + \vec{V}_1\cdot\nabla\eta = W_b \tag{22}$$

$$\eta^{(*)} = \eta^{(t)} + (-\vec{V}_1\cdot\nabla\eta + W_b)\cdot dmt \tag{23}$$

$$\ln(H_1+\eta^{(t+1)}) - \ln(H_1+\eta^{(*)}) = -(\nabla\cdot\vec{V}_1)\cdot dmt. \tag{24}$$

This transformation is used to inhibit the fast increase of gravitational waves and keep

the scheme stable.

We use centered finite difference to treat space variation and will not discuss it further in detail.

The parameters in our model is given in Table 1. u, v, ψ are equal to zero for the continent while they can be calculated for the ocean. As to free sea surface height, in order to keep its continuity, we use the surplus of local pressure and standard pressure to calculate its value at the boundary of the ocean.

Table 1. Model parameters.

$g=9.80$ m/s	$A_m=2.0\times10^5$ m^2/s
$\Omega=7.29\times10^{-5}$ rad/s	$C_D=1.4\times10^{-3}$
$a=6.37\times10^5$ m	$\varepsilon=1.15\times10^{-4}$
$dmt=900$ s	$\Delta\varphi=5°$
$\rho_0=1029$ kg·m^{-3}	$\Delta\lambda=5°$

Firstly, we give the approximate values of u_1, v_1 before computation is done. Then let $u_2 = v_2 = 0$, integrate the equations until the quasi-equilibrium state is obtained.

Ⅲ. EXPERIMENT SCHEME AND DISCUSSION ON THE RESULTS

In this paper we simulate ocean currents in summer and winter respectively using multiyearly averaged pressure and wind fields. Grid size of present model is 5°×5°. The zonal domain of the upper and second layers is from 57.5°S to 57.5°N. The B-Grid is also adopted in difference scheme, which means that the values of u_1, v_1, u_2, v_2 and η are at one point while the wind field, vertical velocities and free sea surface heights are at the points around it. When the changing rate of the total dynamic energy of ocean currents is below 10^{-5}, we consider that quasi-equilibrium state has been obtained.

The main results are as follows.

1. *Free sea surface heights*

The distribution properties of free sea surface height in summer are given in Fig. 1a. It shows that the sea surface in the west is higher than that in the east. So there is a pressure gradient from west to east. Theoretically this pressure gradient plays an important role in pushing and keeping equatorial undercurrents in the second layer. In Southern Hemisphere, except for a small area of low values within the east part of the Atlantic, most of the area in middle latitude is occupied by high values. The simulated sea surface height is very similar to averaged data based on satellite observations between July and October (Stewart, 1985). The difference between the maximum and minimum is 27 cm, which is also close to observation in dimension. The simulated results of IAP ocean model in the Pacific shows that the maxima in Northern and Southern Hemispheres are 46 cm and 74 cm respectively. It seems that the former is closer to observations. Fig. 1a also shows that in the North Pacific the concentrated isolines to the west of maximum center is in accordance with strong currents in that area, which indicates the main property of westward intensification of wind-driven currents. In the Atlantic, this trend manifests itself more clearly.

The wind-driven current theory points out that the northern and southern equatori-

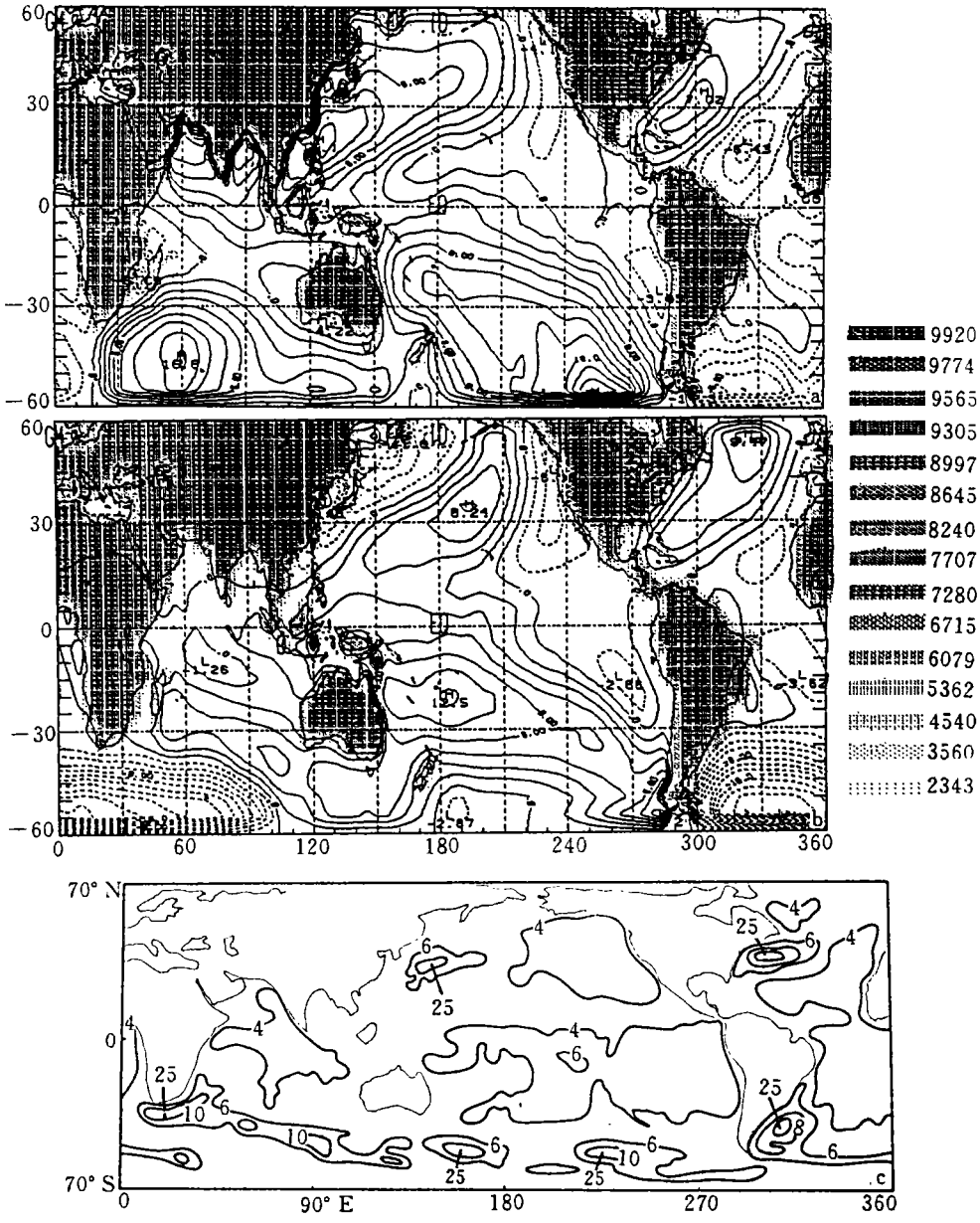

Fig. 1. Simulated free sea surface heights (cm) in summer (a), winter (b) and satellite-observed heights July through October (c).

al currents which are pushed by east wind in tropical areas transport water westward continuously. Owing to the existence of ocean boundary, water is cumulated in that area so that the sea surface in the west is higher than in the east. In addition, the strong currents in the west boundary transport ocean water cumulated in the tropics to higher latitudes so that the middle latitudes is also marked by high water level. The simulated results in this paper are consistent with it.

In winter, the contour of sea surface height is well simulated except for a small area of low values in the west boundary of the Pacific Ocean. However, in the Atlantic Ocean, we have no such low value area. Generally speaking, this result has a bearing on the

winter pressure pattern in this area. That the area is too near to the model boundary is also a reason that is not negligible. According to the theory of statics, if the atmosphere pressure increases 1 hPa, the sea level decreases 1 cm. On the contrary, if the pressure decreases 1 hPa, sea level increases 1 cm. In winter, the east part of Siberian High extends to the west boundary of the Pacific Ocean. So the low level corresponds to the high pressure. In summer, the condition is totally different.

According to the analyses given above, the sea surface height is determined by three factors: sea level pressure, wind field and ocean current. But in a special area, maybe only one factor plays the key role. We also notice that there is no such kind of significant seasonal difference in the west boundary of the Atlantic Ocean. Preliminary investigation shows that it is determined by the difference in intensity and center position between Siberian High and North American High. It also indicates that the Tibetan Plateau as well as the Eurasian mainland are playing an important role in the formation of general circulation of atmosphere and even that of ocean.

2. *Velocity field*

Velocity fields and isolines of stream function are given in Figs. 2a, 2b and Figs. 3a, 3b, respectively. For the purpose of comparison, the observed ocean currents in upper layer are also given in Figs. 4a, 4b. Preliminary comparison shows that they accord with each other very well. The figures show that a warm clockwise cycle is formed in the North Pacific Ocean which is driven by north-east trade wind and west wind. As the zonal domain is from 57.5°S to 57.5°N, only part of the warm water anti-clockwise cycle in

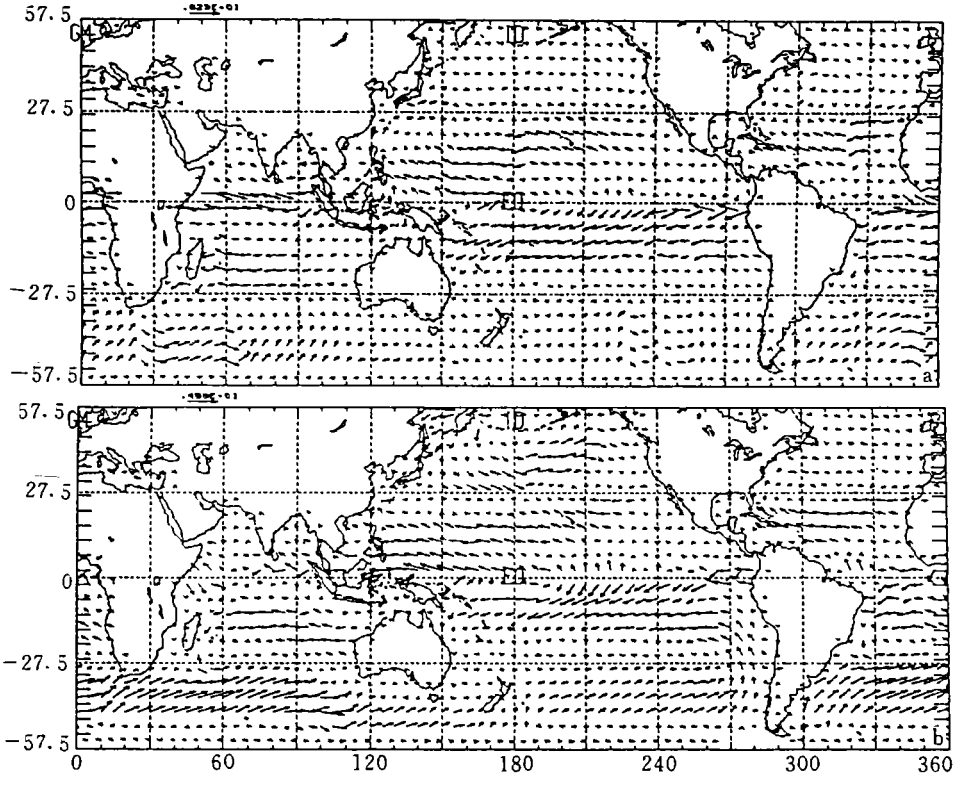

Fig. 2. Simulated ocean sea surface currents in summer (a) and winter (b).

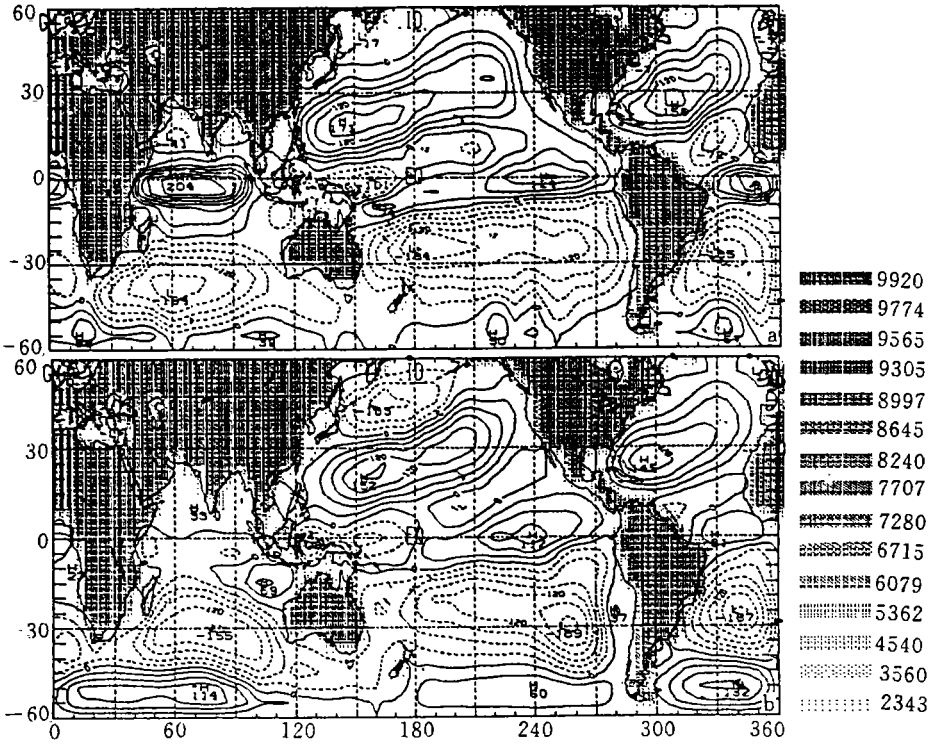

Fig. 3. Stream function of simulated ocean surface currents in summer (a) and winter (b).

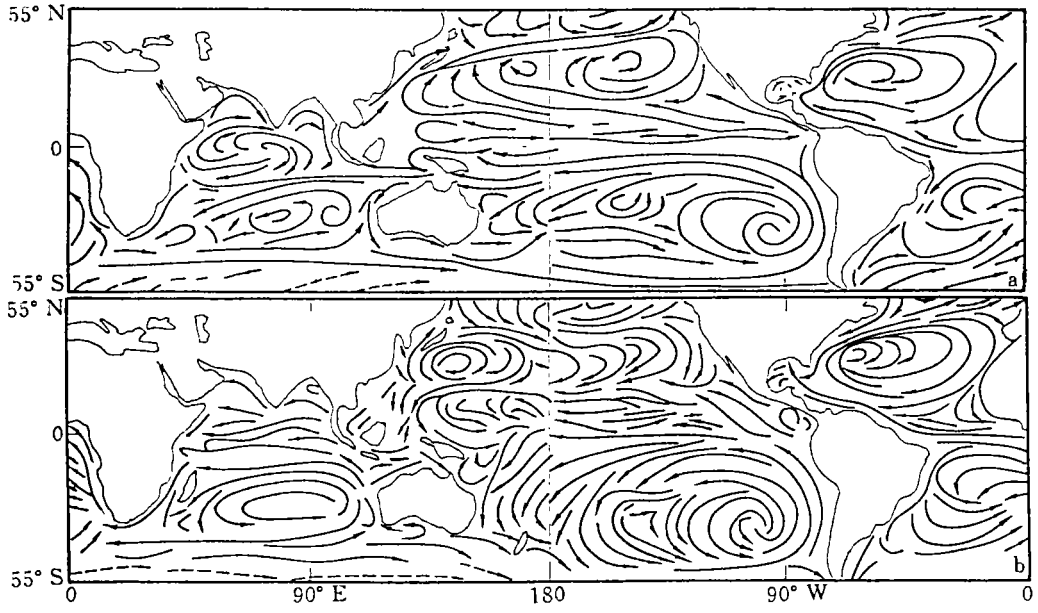

Fig. 4. Observed ocean surface currents in summer (a) and winter (b).

high latitude can be seen from the figure. In the North Indian Ocean, surface currents is westward in winter while it is eastward in summer. This kind of seasonal variation is also well simulated in our model.

However, there are some minor differences between simulation and observation. Only part of the equatorial counter currents can be seen from the figure. The isoline of

stream function of surface currents (Fig. 3) shows an area of negative values along the equator in north-east part of the Pacific Ocean which indicates surface flow from west to east. But there are no simulated equatorial counter currents in OSU OGCM. On the contrary, Ekman transportation is more significant in OSU model. Surface flows of subtropical area in the East Pacific are perpendicular to wind stress and point to west (Northern Hemisphere) and east (Southern Hemisphere) respectively (Ni, 1993, and see Fig. 5a). The difference between two models is determined by their design: OSU OGCM using rigid-lid approximation neglects surface height variation and gives simulated surface currents some characteristics of Ekman flow because wind stress is the prime factor with this simplification. The model developed in this paper includes surface height variation so that the surface fluid is influenced by Coriolis force, wind stress and horizontal pressure gradient force collectively while the second layer is determined by Coriolis force and pressure gradient force which gives it some significant characteristics of geostrophic flow. However, the Ekman transportation plays an important role in inner region and east boundary of the basin in our model so that observed east boundary flows such as California, Humbolt and Benguela currents are not simulated fully and California current would deviate to the north too much.

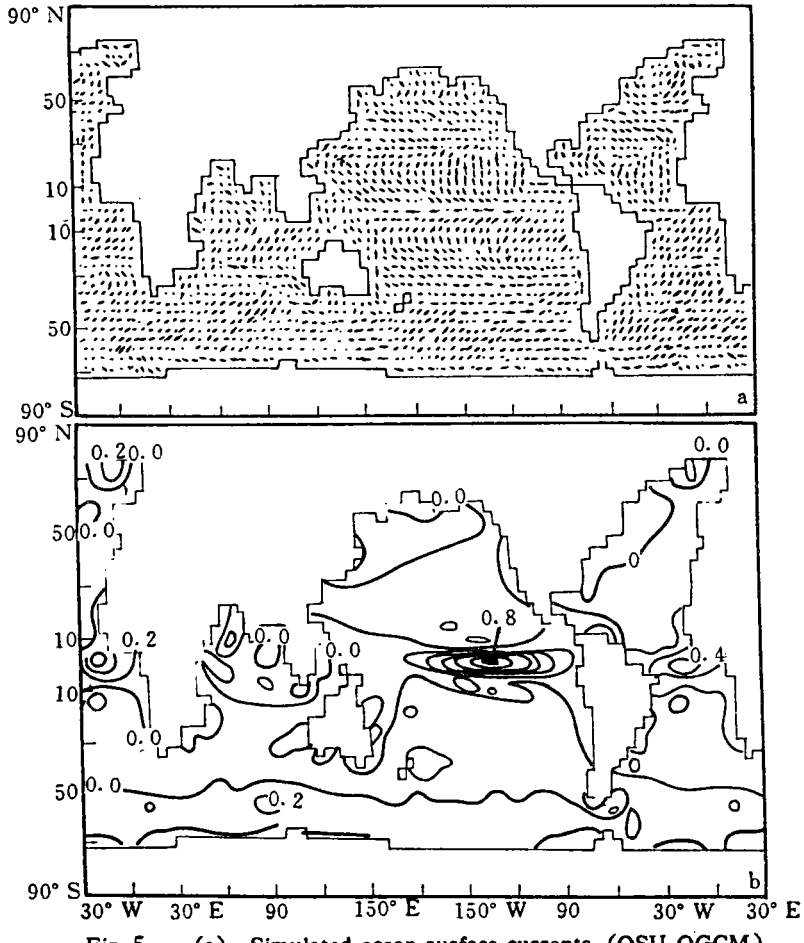

Fig. 5. (a). Simulated ocean surface currents (OSU OGCM)
(b). Simulated vertical velocity (m/day) (OSU OGCM)

The general circulation of ocean water in the second layer is simple and shows a significant characteristic of geostrophic flow. Only part of eastward undercurrents appear in our simulation but the characteristic of convergence is very significant in equatorial zone. In Indian Ocean, although observation shows that there are undercurrents when northeast wind is prevalent (Leetma, McCreary, Moore, 1980), we cannot find any corresponding undercurrents in the simulated results.

3. *Divergence field*

In order to illustrate the divergence of simulated ocean currents, the vertical velocities between two layers are given in Fig. 6. It is shown that the strong upwelling in narrow tropical area in contrast to weak downwelling in a wider region is mainly driven by surface winds. These vertical flows indicate the convergence of equatorial currents and divergence of other surface currents. However, the simulated values are slightly higher than those of observation. It is mainly caused by the model design. In middle east part of the Pacific Ocean which belong to boreal subtropical zone, simulated ocean currents point to north-west while the observed currents to the west-northwest. It causes strong Ekman divergence and upwelling in this area. OSU OGCM with rigid-lid approximation exaggerated it further more and got stronger upwelling in equatorial area than our model (Fig. 5b).

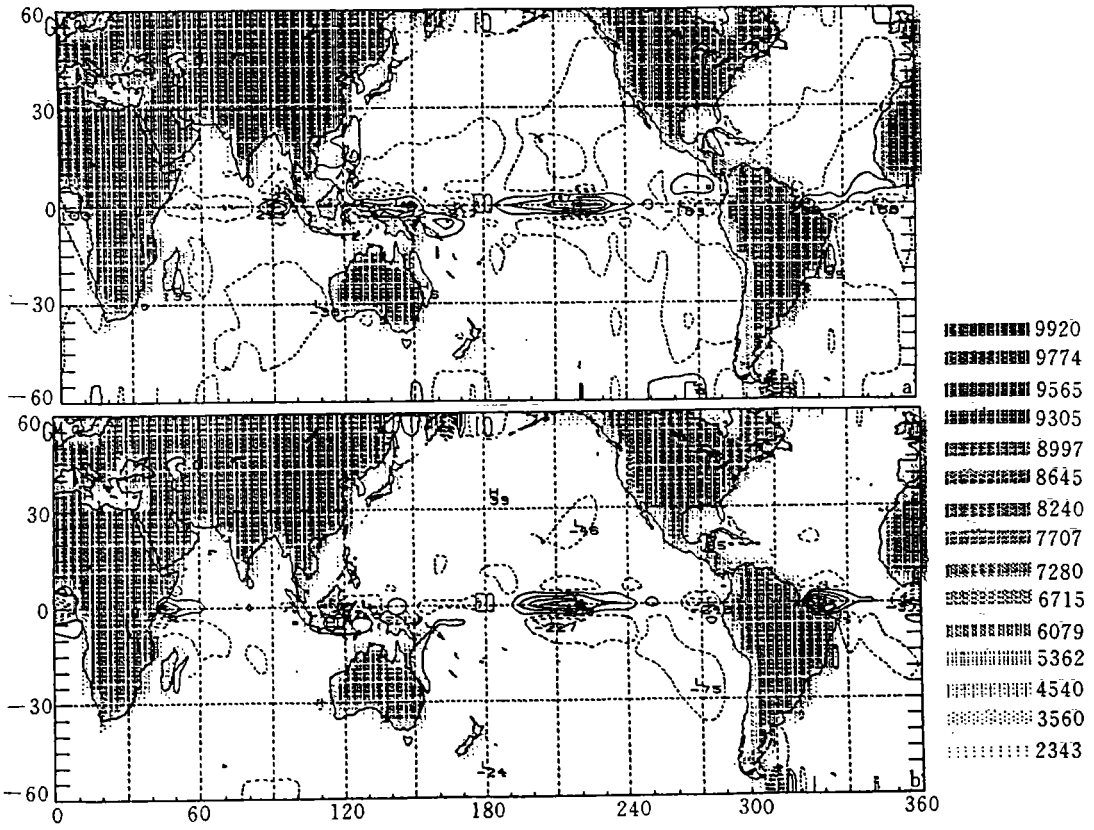

Fig. 6. Simulated vertical velocity (unit: 10^{-6} cm/s) in summer (a) and winter (b).

Reasonable upwelling in equatorial area has its significance. Narrow but strong upwelling along the equator and spacious downwelling in other areas cause mass trans-

portation between two layers and consist with divergence and convergence characteristics in surface layer. Downwelling in subtropical ocean is also necessary for the transportation of anticyclone eddies to the second layer. However, too strong upwellings distort real situation of ocean currents and destroy simulation results.

Ⅳ. CONCLUSIONS

Ocean currents in winter or summer can be simulated using two-layer primitive equation model developed in this paper. Thus, when it is coupled with AGCM, we can use simulated ocean currents to calculate advective terms in the predictive equation of surface temperature.

Preliminary comparisons between the simulated results and those of OSU OGCM and IAP OGCM show that the difference between our model and those multi-layer models can be neglected as to the simulation on seasonal variations of ocean currents in the first and second layers. In other words, the simulated ocean currents in this model can be used for calculating advective terms in the predictive equation of surface temperature. However, there are some minor differences between simulation and observation. These differences mainly appear at the boundary of the basin. Only part of the undercurrents in equatorial area can be seen from the simulated results. Low resolution may be the primary cause. The equatorial undercurrents play the key role in ENSO and related abnormal climate phenomena. We plan to improve the resolution by the use of different scheme in equatorial zone in the future. After that, we can couple it with other areas to improve the simulations on equatorial undercurrents in this area.

Generally speaking, the two-layer primitive model developed in this paper with simple construction and clear physical mechanism can be coupled with AGCM to do some research work on short-term climate variations.

REFERENCES

Leetma A, McCreary J P Jr, Moore D W, 1980. Equatorial currents: Observations and Theory. In Evolution of Physical Oceanography. eds. B. A. Warren and C., Wunch, The MIT Press, Cambridge, MA, 184-196.

Ni Yunqi, 1993. Climate Dynamics. Beijing: Meteorology Press. 546-547. (in Chinese)

Qian Yongfu, Wang Qianqian, 1994. Numerical calculations of sea surface winds and ocean surface currents in winter and summer. *Journal of Tropical Meteorology*. **10**: 212-221 (in Chinese).

Stewart R H, 1985. Methods of satellite Oceanography. University of California Press. 251-252.

Zeng Q C, Yuan C G, Zhao J P, 1992. Proceedings of symposium on ocean circulation. Beijing: Ocean Press. 23-24. (in Chinese)